Fits to the spectra of broad-line region of active galactic nuclei and opacities for two-photon pair production

M. Ntshatsha[*]

Centre for Astro-Particle Physics (CAPP) and Department of Physics, University of Johannesburg, Auckland Park 2006, South Africa
E-mail: mfuphin95@gmail.com

S. Razzaque

Centre for Astro-Particle Physics (CAPP) and Department of Physics, University of Johannesburg, Auckland Park 2006, South Africa
E-mail: srazzque@uj.ac.za

R.J. Britto

University of the Free State, PO Box 339, Bloemfontein 9300, South Africa
E-mail: dr.richard.britto@gmail.com

Based on the spectral analysis of a composite Hubble Space Telescope (HST) spectrum made of 184 quasar data, we model the emission lines of the broad-line region (BLR) using analytic functions. For simplicity of this paper we neglect effects of the continuum emission, which may be resulting from emission by the accretion disk, and assume the emission of the BLR to be composed of the most prominent emission lines that form as a result of ionization and recombination processes within regions of the BLR. We also calculate opacities for gamma-rays propagating in the BLR and interacting with the modeled emission to produce electron-positron ($e^{\pm}$) pairs.

High Energy Astrophysics in Southern Africa - HEASA2018
1-3 August, 2018
Parys, Free State, South Africa

---

[*]Speaker.

1. Introduction

Since their discovery in the 1960s [1] the superluminal properties of active galactic nuclei (AGN) have prompted astrophysicists to probe more into these objects. AGN are characterised into a variety of classes, however, the basic structure of all AGN is the same according to the unified model of AGN [2]. In the picture of the unified model is a supermassive black hole at the center of the AGN fueling the emission processes. Some radial distance away from the black hole is a torus of dusty/molecular clouds from which gas is being pulled by the gravitational force of the black hole. In the process of in-fall of the gas it accumulates as a thin disk of gas around the black hole, called the accretion disk or just simply disk. Across a large radial range of the disk, wind outflow processes from the disk contribute to the formation of the BLR close to the disk [3], (a distance in the order of light years from the black hole [4]). Further away from the outer edge of the BLR, where there exists an apparent gap, is the narrow line region (NLR) [5]. There are clear distinctions between the BLR and the NLR, observable mainly by considering the full width at half maximum (FWHM) of their spectral lines ($\sim$ 4000 km/s and $\sim$ 500 km/s, respectively [5]). Both the BLR and NLR radii, (R_{BLR}, R_{NLR}), scale as $\sim L^{1/2}$, where L is the luminosity of the central source. However, they do differ in radius and covering factor where $R_{NLR} \sim (10-100)$ pc with covering factor of about 2% [5], in comparison to $R_{BLR} \sim (0.1-1)$ pc [4] with a covering factor of $(5-30)$% [5].

The γ-ray spectra of quasars can be typically described by a simple power-law, however, in some blazar spectra they break away from the trend of the power-law at certain γ-ray energies. With these breaks at specific energies, models such as the broken power-law or log-parabola then become better functions that physically describe both ends of the spectrum at enegies lower and higher than this break energy [4]. It was shown by [4, 6] that the break energies in some blazar spectra are consistent with the absorption of γ-ray photons by some emission lines in the BLR through $e^{\pm}$ pair production. To calculate this absorption detailed information about the distribution of the target photon gas is required [7].

In this proceedings we investigate the absorption of γ-rays propagating through the BLR in bright AGN. We model the BLR by fitting the most visible emission lines obtained from the composite spectrum of HST [8]. By modeling the BLR in this way we aim for a more realistic description of its photon distribution across its entire emission range. Finally we calculate the opacity of the BLR for γ-rays in the energy range 90 MeV – 400 GeV.

2. Data Analysis

We use the HST data of a composite spectrum of 332 spectra of 184 quasars composed of both radio loud and radio quiet AGN. We plotted data[1] from Figure 1 of [8] by converting the relative flux F_λ in the $(303-4989)$ Å wavelength range into a F_ε relative flux in the $(2.48-41.0)$ eV energy range. In the composite HST quasar data composed and studied by [1] they showed that in the wavelength range $(350-3000)$ Å there is a distinct change in the shape of the continuum. They reported power law indices of ~ -2 in the extreme ultraviolet (EUV) region $\sim (300-1052)$ Å and ~ -1 in the near ultraviolet (NUV) region $\sim (1052-3000)$ Å. With this change in the power law index they concluded that the quasar UV spectral continuum can be approximated with a broken

---

[1]ASCII file provided by R. C. Telfer

power law (BPL). In the work of [8] they show that the same pattern is observed for subset samples of radio loud and radio quiet quasars. In fitting the continuum of the composite spectrum we then followed [1, 8] by fitting it with a broken power law $\propto (\varepsilon/\varepsilon_B)^{-\beta_j}$ with $j = 1, 2$ below and above the break energy ε_B respectively. However, instead of fitting it using the IRAF task *specfit* in the wavelength windows chosen in [8], we rather "hand"-fitted the continuum over almost the entire UV range of the HST data file , $(303 - 4989)$ Å, where we have excluded 12 data points $(291 - 302)$ Å which had large errors associated with them. In so doing we obtained power-law indices $\beta_1 = -1.35$ and $\beta_2 = -0.18$ below and above the break energy $\varepsilon_B = 9.8$ eV respectively. We note here that at the low wavelengths (< 560 Å) the composite spectrum is composed of less than 10 spectra contributing to the composite at a given wavelength, as it is mentioned in [8]. From this point (< 560 Å) there is a slight hardening of the continuum, deviating from the power law [8]. It is noteworthy to mention that the small number of contributing spectra in this wavelength range may be the cause of this deviation and for this reason the hardening here may not necessarily be characteristic of all quasars [8]. The emission lines in this region, however, are real and reflect high signal to noise ratio data obtained to study the He II Gunn-Peterson effect [8]. Above 900 Å, any deviation from the power law is caused by weak emission features, particularly Fe II [1]. At wavelengths above 2200 Å these features are most prominent that they cause the continuum shape to deviate quite significantly from the power law. However, in this proceedings we attempt to aim for the full representation of the BLR across all its emission. To achieve this we performed a fit over the wavelength range $(303 - 4989)$ Å, effectively representative of the whole UV range of the BLR spectrum of quasars.

To fit the BLR emission lines it was convenient to remove the continuum by subtracting the fitted BPL from the data. Each emission line from a given frequency range was isolated and independently fit with either the Breit-Wigner (BW) for lines with a narrow profile, the Gaussian (Ga) for lines with a broad profile or a combination of the two if the profile of a line had prominent broad and narrow components. The emission lines are each fitted individually, however, due to the high density of some emission features in the range below the peak labeled λ 2085, the so-called 3000 Å bump ($\approx 2200 - 4000$) Å [9], we use the Smoothly-joint Broken Power Law (SBPL) as an average estimate of the combined emission of the lines appearing in the energy range $(3.35 - 4.09)$ eV, labeled as λ_B 3205 and $(4.60 - 5.50)$ eV labeled λ_B 2459. Other ranges averaged over with the SBPL are $(18.5 - 20.6)$ eV labeled λ_B 640, $(22.1 - 26.8)$ eV λ_B 474, $(28.1 - 34.6)$ eV λ_B 404 and $(34.6 - 39.4)$ eV λ_B 328, where the subscript B signifies the position of the break chosen in the SBPL. It is not the position of the specific line. Many of the lines fitted in this proceedings are not identified, especially below the Lyman limit (912 Å) and although the composite spectrum considered here is representative of the BLR behaviour of a typical quasar, it may not necessarily be the case that all the lines considered in this proceedings will appear in all quasars. The composite simply suggests hints of the existence of these lines, which we consider for completeness and without loss of generality. The functions used for fitting are expressed as

$$BW(\varepsilon) = \frac{n_i}{2\pi} \frac{w_i}{(\varepsilon - \varepsilon_i)^2 + (w_i/2)^2} \tag{2.1}$$

$$SBPL(\varepsilon) = \frac{n_i}{\varepsilon_i} \left[\left(\frac{\varepsilon}{\varepsilon_i} \right)^{\alpha_1} + \left(\frac{\varepsilon}{\varepsilon_i} \right)^{\alpha_2} \right]^{-1} \tag{2.2}$$

$$Ga(\varepsilon) = \frac{n_i}{\varepsilon_i} \exp\left[-\left(\frac{\varepsilon - \varepsilon_i}{\sqrt{2}w_i} \right)^2 \right] \tag{2.3}$$

where

$$n_i[\text{cm}^{-3}] = 1.66 \times 10^{11} \left(\frac{R_{BLR}}{10^{17}\text{cm}} \right)^{-2} \left(\frac{\varepsilon_i}{\text{eV}} \right)^{-1} \left(\frac{k_i L_{\text{Ly}_\alpha}}{10^{45}\text{erg/s}} \right) \tag{2.4}$$

k_i is the fraction of the luminosity of the ith line relative to the luminosity of the Ly$_\alpha$ line. L_{Ly_α} in the above equations is the luminosity of Ly$_\alpha$. The Ly$_\alpha$ line was fitted as a linear combination of the BW and Ga, the k_i for the Ga component was taken to be 33% that of the BW component. All the lines in the fits are then normalized by the k_i of the BW component of Ly$_\alpha$. ε_i is the peak energy of the ith line and w_i is the energy width of the line. n_i is the density of photons emitted by the ith line, where we make the crude assumption that the emission lines appear at the same radius within the BLR, so that there is no variation in photon density. In reality, different emission lines originate from different regions of the BLR and the photon density varies with radius. A detailed calculation in future will need to include this effect while calculating the γ-ray opacity. The indices α_1 and α_2 describe the steepness of the rise and fall of a line before and after the peak energy ε_i respectively. To estimate the size of the BLR we use its scaling $R_{BLR} \approx 10^{18}L_{disk,47}^{1/2}$ cm [6] [2]. Since the BLR reprocesses a fraction of the disk emission in both its lines and continuum [10] we take the luminosity of the BLR, $L_{BLR} = 0.1L_{disk}$ to be a fraction of the disk luminosity [11] as it is treated in one of the cases in the works of [10]. From Table 1 of [8] we get the average disk luminosity of $10^{46.16}$erg/s corresponding to a BLR size of $R_{BLR} \approx 12.02 \times 10^{17}$cm for the composite spectrum. The peak energies ε_i of most of the lines were obtained from Table 1 in [8] and kept fixed, but in some cases we needed to shift them to match the data. The equivalent widths of the lines were also held fixed and all the values (with the exception of the Ga component in the Ly$_\alpha$ fit) of the parameter k_i used in the fits were kept free and obtained using the *scipy.optimize.curve_fit* optimization package in python. The indices (α_1, α_2) were held fixed for lines and regions where *curve_fit* gave either infinities for the errors in the parameters, or error values larger than the parameters. Instances where the indices were free are indicated with an asterisk in Table 1. The *scipy.optimize.curve_fit* function optimizes and determines fit parameters of a given model by using least squares minimization. To get a quantitative measure of the goodness of the fit we calculated a reduced χ^2_{red} on each trial. The lowest χ^2_{red} obtained was 4.2 with 4639 degrees of freedom for the fit presented here. The fit parameters together with the model used are tabulated in Table 1. Figure 1 a) shows the plot (in red) of the fit imposed on the BLR composite data, where Figure 1 b) in the bottom panel is a plot of the residual calculated as shown in the figure.

Next we calculate the opacities of $e^{\pm}$ pair creation by γ-rays interacting with the BLR photons. We used the standard opacity formula from [12] and adapted it for the fitting functions as:

---

[2]In this notation $L_{disk} = 10^{47}L_{disk,47}$ erg/s is the accretion disk luminosity.

Table 1: Parameter list and model used in fitting the spectral lines of the quasar spectrum.

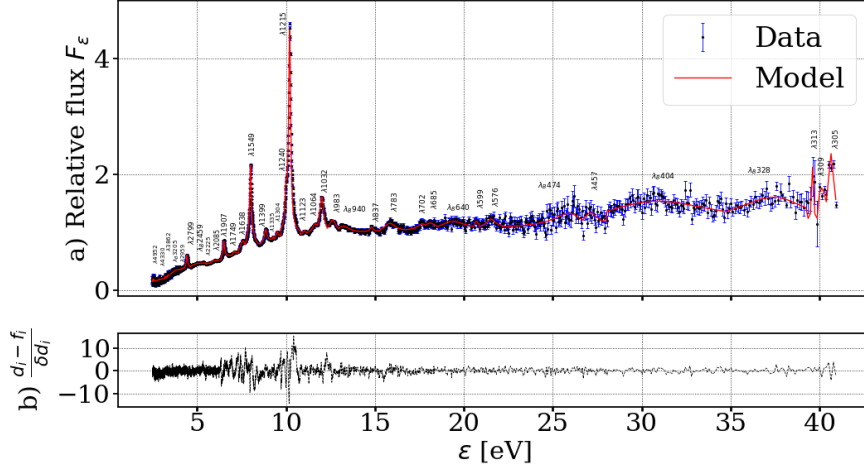| Line / energy range	Function	k_i	Line peak energy ε_i [eV] (Fixed)	Line width w_i [eV] (Fixed)	α_1 (Fixed)	α_2 (Fixed)
[O III] λ 4952	BW	1.41×10^{-4}	2.50	0.008		
Hβ λ 4857	BW	4.18×10^{-4}	2.55	0.02		
Hγ λ 4330	BW	2.90×10^{-5}	2.86	0.003		
[Ne III] λ 3862	BW	1.70×10^{-4}	3.21	0.009		
[O II] λ 3723	BW	7.71×10^{-4}	3.33	0.03		
λ_B 3205	SBPL	3.15×10^{-1}	3.87		13.2	-12.8
Fe II λ 2959	BW	2.53×10^{-2}	4.19	0.36		
Mg II λ 2799	BW	8.29×10^{-3}	4.43	0.056		
	Ga	3.03×10^{-1}	4.43	0.14		
λ_B 2459	SBPL	5.14×10^{-1}	5.04		15.2	-8.8
Fe II λ 2225	Ga	6.47×10^{-2}	5.57	0.25		
Fe III λ 2085	BW	8.79×10^{-3}	5.95	0.25		
C III + Si III]	BW	3.04×10^{-2}	6.50	0.09		
λ 1907	Ga	2.66×10^{-1}	6.50	0.2		
N III] λ 1749	BW	1.40×10^{-2}	7.09	0.16		
λ 1638 possibly He II	BW	9.07×10^{-2}	7.57	0.32		
C IV λ 1549	BW	1.87×10^{-1}	8.00	0.0995		
	Ga	2.25	8.00	0.19		
Si IV + O IV] λ 1399	BW	7.02×10^{-2}	8.86	0.173		
C II λ 1335	BW	3.64×10^{-3}	9.29	0.041		
O I + Si II λ 1304	BW	2.43×10^{-2}	9.51	0.12		
N V λ1240	BW	1.50×10^{-1}	10.0	0.129		
Ly α λ 1215	BW	1	10.20	0.14		
	Ga	0.33	10.20	0.82		
Fe III λ 1123	BW	2.73×10^{-2}	11.04	0.18		
Ar I λ 1064	BW	1.71×10^{-1}	11.65	0.42		
O VI + Ly β λ 1032	BW	4.15×10^{-1}	12.01	0.27		
C III + N III λ 983	BW	2.77×10^{-1}	12.61	0.48		
H I + Ly series +S VI λ_B 940	SBPL	5.05	13.19		42.77	-49.84
O III λ 837	BW	4.69×10^{-2}	14.81	0.2		
Ne VIII + O IV λ 783	SBPL	8.19	15.83		59.99	-59.97
λ 702	BW	2.11×10^{-1}	17.66	0.594		
λ 685	BW	2.85×10^{-1}	18.1	0.7		
λ_B 640	SBPL	12.03	19.4		37.12	-37.10
λ 599	BW	$1.40\times^{-1}$	20.7	0.3		
λ 576	BW	3.74×10^{-1}	21.53	0.594		
λ_B 474	SBPL	32.81	26.16		64.83*	-26.40*
λ 457	BW	1.03	27.1	0.91		
λ_B 404	SBPL	91.84	30.69		11.28*	-12.03*
λ_B 328	SBPL	144.37	37.80		30.31*	-17.53*
λ 313	BW	6.80×10^{-1}	39.61	0.093		
λ 309	BW	2.65	40.12	0.594		
He II Ly$_\alpha$ λ 305	BW	3.33	40.65	0.356		

Figure 1: a) Fit of the emission lines extending from $(2.48 - 41.0)$ eV of the BLR spectrum (solid red line). b) Plot of the residual at each ε. On the y-axis of the bottom panel the symbols $d_i, f_i, \delta d_i$ are the ith data point, model evaluated at the ith point and the error on the ith data point, respectively.

$$\frac{d\tau_{BW}}{dx} = \frac{r_0^2}{2}\left(\frac{m_e^2 c^4}{E(1+z)}\right)^2 \sum_i n_i w_i \int_{\frac{m_e^2 c^4}{E(1+z)}}^{\infty} \frac{\bar{\phi}[s_0(\varepsilon)]}{\varepsilon^2[(\varepsilon-\varepsilon_i)^2 + (w_i/2)^2]} d\varepsilon \tag{2.5}$$

$$\frac{d\tau_{SBPL}}{dx} = 1.3\pi r_0^2\left(\frac{m_e^2 c^4}{E(1+z)}\right)^2 \sum_i \frac{n_i}{\varepsilon_i} \int_{\frac{m_e^2 c^4}{E(1+z)}}^{\infty} \frac{\bar{\phi}[s_0(\varepsilon)]}{\varepsilon^2[(\varepsilon/\varepsilon_i)^{\alpha_1} + (\varepsilon/\varepsilon_i)^{\alpha_2}]} d\varepsilon \tag{2.6}$$

$$\frac{d\tau_{Ga}}{dx} = 1.5\pi r_0^2\left(\frac{m_e^2 c^4}{E(1+z)}\right)^2 \sum_i \frac{n_i}{\varepsilon_i} \int_{\frac{m_e^2 c^4}{E(1+z)}}^{\infty} \frac{\bar{\phi}[s_0(\varepsilon)]}{\varepsilon^2 \exp\left[\left(\frac{\varepsilon-\varepsilon_i}{\sqrt{2}w_i}\right)^2\right]} d\varepsilon \tag{2.7}$$

where equation (2.5) is taken from [11], the factors in front of equations (2.6), (2.7) are the ratios of the area under the curves BW/SBPL and BW/Ga, and n_i is the quantity referred to by equation (2.4), $\bar{\phi}[\nu] = \int_1^{\nu} s\bar{\sigma}_{\gamma\gamma}(s)\,ds$, $s_0(\varepsilon) = \varepsilon E/m_e^2 c^4$, $\bar{\sigma}_{\gamma\gamma} = 1/s\left[(2+2/s - 1/s^2)\ln\frac{1+\beta}{1-\beta} - 2\beta(1+1/s)\right]$ is the dimensionless photon cross-section where $\beta^2 = (1 - 1/s)$, m_e is the elemental electron mass, r_0 is the classical electron radius, z is the redshift and ε, E are the target photon, gamma photon energies respectively. We calculate the opacities by taking the radius of the BLR as $R_{BLR} = 12.02 \times 10^{17}$cm as inferred by [6]. The opacities of the fitted emission lines are shown in Figure 2, with the blue dot-dash line being the sum of the line opacities.

In the delta function approximation for $\gamma\gamma$ absorption the opacity is given by:

$$\tau_{\gamma\gamma}(L_i, \varepsilon_i) = \frac{L_i}{4\pi c R_{BLR}\varepsilon_i}\frac{\sigma_T}{5} \approx 16.5\left(\frac{L_i}{9.2\times 10^{44}\text{ erg/s}}\right)\left(\frac{R_{BLR}}{1.2\times 10^{18}\text{ cm}}\right)^{-1}\left(\frac{\varepsilon_i}{10.2\text{ eV}}\right)^{-1} \tag{2.8}$$

which is the opacity for the Ly$_\alpha$ line, L_i and σ_T are the line luminosity and the Thomson cross-section, respectively.
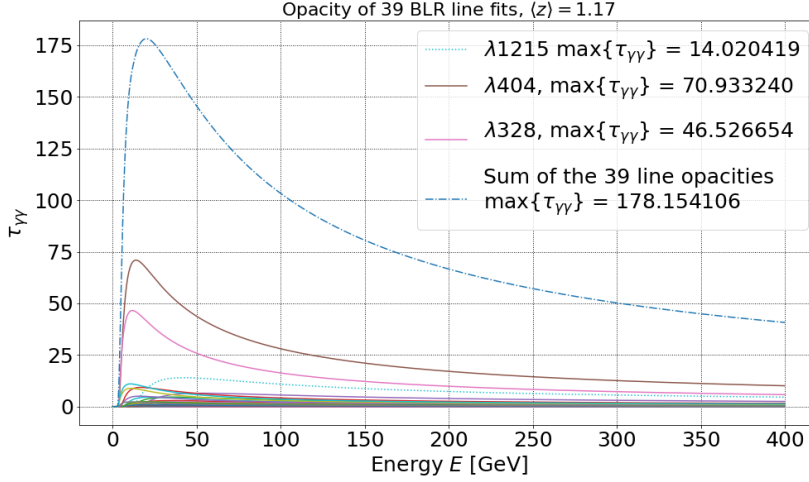
Figure 2: Opacity of BLR lines identified in the composite spectrum of 184 quasars. The blue dot-dash line is the sum of the individual line opacities.

3. Summary and Discussion

The careful analysis of a large sample of quasar spectra spanning a large range in redshift $0.33 < z < 3.7$ done by [8] has made it possible to model the emission of the BLR lines. The BW, SBPL and Ga functions were used to individually fit the peaks of the quasar data and the data was well reproduced by the fits with $\chi^2_{red} = 4.2$. The modeling of these lines gives a reasonable description of the BLR and a good opacity estimate of γ-ray photons in the BLR. The maximum opacity summing of all the emission lines came to the value of $\tau \sim 178$ at ~ 18.9 GeV. This threshold energy is nearly consitent with that of the 20 GeV breaks due to H LyC in many blazars reported by [6]. At $\tau \sim 178$, the opacity sum of the whole composite is quite high and this is due to the high density of the emission lines in the EUV which are averaged over with the SBPL, in particular the λ_B 404 and λ_B 328 regions. And as it has already been hinted in section 2 by a slight hardening of the continuum at low wavelengths, this behaviour may not necessarily be representative of all quasars since only few quasar spectra contributed to the composite spectrum at these wavelengths. However, if this slight hardening of the spectrum at these wavelengths happens to be real in a typical quasar, then the calculated opacity over these regions of multiple emission lines (λ_B 404, λ_B 328) suggests a strong dominance of EUV photons in attenuating γ-rays even more than the Ly$_\alpha$ line, as can be seen in Figure 2. The peak opacity value of the Ly$_\alpha$ line was ~ 14.0 at ~ 43.0 GeV, and the λ_B 404 and λ_B 328 were ~ 70.9 and ~ 46.4 at ~ 13.5 GeV and ~ 10.8 GeV, respectively. Using the delta function approximation in equation (2.8), the opacity of Ly$_\alpha \sim 16.5$, while it is ~ 15.4 when using equation (2) from the [4, 6] papers. Note that the absorption of the γ-ray photons depends on the location of the γ-ray emitting zone in the BLR. In case the γ-ray emitting zone is located outside or closer to the outer edge of the BLR, the opacity would be negligible or a fraction of the values we calculate here [11]. In addition to $e^{\pm}$ pair-production-related spectral breaks, the spectra of many blazars show dips in the $\gtrsim 10$ GeV range as can be seen in the literature [4, 6, 13]. It seems, therefore, reasonable that the lines that have significant absorption at $E \sim 50$ GeV would

cause the dips observed beyond the spectral break of blazars. The calculated opacity of the BLR of blazars opens the possibility of constraining the emission zone of the γ-rays produced in the jets of AGN via the transmission function. We suggest that by modeling the BLR and including Galactic background radiation and their respective opacities it will be possible to locate the γ-ray emission zone.

4. Acknolwdgements

References

[1] W. Zheng, G.A. Kriss, R.C. Telfer, J.P. Grimes and A.F. Davidsen, *A composite HST spectrum of quasars*, The Astrophysical Journal **475**(2) (1997) p.469

[2] M. C. Urry and P. Padovani, *Unified schemes for radio-loud active galactic nuclei*, Publications of the Astronomical Society of the Pacific, **107**(715) (1995) p.803.

[3] B. Czerny and K. Hryniewicz, *The origin of the broad line region in active galactic nuclei*, Astronomy & Astrophysics **525** (2011) p.L8.

[4] J. Poutanen and B. Stern, *GeV breaks in blazars as a result of gamma-ray absorption within the broad-line region*, The Astrophysical Journal Letters **717**(2) 2010 p.L118.

[5] H. Netzer and A. Laor, *Dust in the narrow-line region of active galactic nuclei*, The Astrophysical Journal **404** (1993) pp.L51–L54.

[6] B.E. Stern and J. Poutanen, *The mystery of spectral breaks: Lyman continuum absorption by photon-photon pair production in the Fermi GeV spectra of bright blazars*, The Astrophysical Journal **794**(1) (2014) p.8.

[7] R.J. Gould and G.P. Schréder, *Opacity of the universe to high-energy photons*, Physical Review **155**(5) (1967) p.1408.

[8] R.C. Telfer, W. Zheng, G.A. Kriss and A.F. Davidsen, *The rest-frame extreme-ultraviolet spectral properties of quasi-stellar objects*, The Astrophysical Journal **565**(2) (2002) p.773.

[9] D.E. Vanden Berk, G.T. Richards, A. Bauer, M.A. Strauss, D.P. Schneider, T.M. Heckman, D.G. York, P.B. Hall, X. Fan, G.R. Knapp, and others, *Composite quasar spectra from the sloan digital sky survey*, The Astronomical Journal **122**(2) (2001) p.549

[10] G. Ghisellini and F. Tavecchio, *Canonical high-power blazars*, Monthly Notices of the Royal Astronomical Society **397**(2)(2009) pp. 985–1002

[11] R.J. Britto, S. Razzaque and B. Lott, *Spectral Studies of Flaring FSRQs at GeV Energies Using Pass 8 Fermi-LAT Data*, arXiv preprint arXiv:1502.07624 (2015)

[12] R.J. Gould and G.P. Schréder, *Pair production in photon-photon collisions*, Physical Review **155**(5) (1967) p.1404.

[13] L. Costamante and S. Cutini and G. Tosti and E. Antolini and A. Tramacere, *On the origin of gamma-rays in Fermi blazars: beyondthe broad-line region*, Monthly Notices of the Royal Astronomical Society, **477**(4) (2018) pp. 4749–4767.